Liquid Crystalline Side Chain Polysiloxanes with 4-Amino-4′-stilbenecarboxylic Ester Mesogens

Marietta O. Bautista,† Randolph S. Duran,‡ and Warren T. Ford*,†

Departments of Chemistry, Oklahoma State University, Stillwater, Oklahoma 74078-0447, and University of Florida, Gainesville, Florida 32611-2046

Received July 23, 1992; Revised Manuscript Received October 8, 1992

ABSTRACT: Side chain polysiloxanes with 4-(dimethylamino)- and 4-[4-(hexyloxy)piperidino]-4′-stilbenecarboxylic ester mesogens were synthesized from poly(hydromethylsiloxane) and poly(hydromethylsiloxane-*co*-dimethylsiloxane) and the 10-undecen-1-yl esters. Size exclusion chromatography (SEC) underestimates M_n of the (dimethylamino)stilbene homopolymer by a factor of 4 and M_n of the piperidinostilbene homopolymer by a factor of 2 compared with ^{1}H NMR end group analyses. SEC and NMR values of M_n approximately agree for the copolymers. The phases of the monomers and polysiloxanes were assigned by polarizing microscopy and X-ray diffraction. The copolysiloxanes have T_g near −40 °C by DSC, but T_g was not detected for the homopolysiloxanes. Both homopolysiloxanes have nematic phases, and both copolymers have S_A phases. The [(hexyloxy)piperidino]stilbene polymers have more ordered phases, assigned as S_B of the copolymer and either S_B or hexagonal nematic of the homopolymer. The isotropic transitions were detected by polarizing microscopy but not by DSC. All of the polysiloxanes form stable monolayers on water that can be compressed to mean areas per stilbene repeat unit ranging from 23 to 34 Å^2 and to pressures of ≥50 mN/m.

Introduction

Organic compounds, polymers, and liquid crystalline polymers (LCPs) have generated considerable interest as potential materials for nonlinear optical (NLO) applications.[1] Since a second-order NLO material must be noncentrosymmetric, films of glassy NLO polymers are usually ordered in a dc electric field. However, films of NLO-active compounds dissolved in polymers such as poly(methyl methacrylate) lose their NLO activity over hours or days at room temperature, far below T_g, because of molecular and polymer chain motion in the glassy state.[2-7] Lack of temporal stability is a problem also with the NLO-active groups covalently bound to PMMA and polystyrene.[8-13] Much improved temporal stability has been achieved by orienting and covalently bonding the NLO-active groups into cross-linked networks.[14-21] Our approach to stable NLO polymers is to orient them in a high-temperature liquid crystalline phase and cool them to anisotropic room temperature glassy states. The order achieved in the electric field may be retained longer if the stable state of the polymer at room temperature is anisotropic. Thus, our aim is to prepare high-T_g side chain liquid crystalline polymers (SCLCPs).[22]

SCLCPs with polarizable aromatic mesogens are good candidates for thin-film second-order NLO materials. Most previously reported side chain second harmonic generation (SHG) polymers have the donor substituent in the spacer chain and the acceptor at the end of the side chain.[23-32] Methyl methacrylate polymers with 4-alkoxy-4′-(alkylsulfonyl)stilbene side chains, which are transparent down to 410 nm, resulted in a reasonably high nonlinearity (d_{33} ≤ 9 pm/V).[33,34] Our earlier LC side chain polyacrylates with polarized 4-(dimethylamino)-4′-stilbenecarboxylic ester mesogens (**1**),[35] having the donor substituent at the end of the side chain and the acceptor in the spacer chain, form optically clear thin films, and one of them exhibited a strong SHG response.[36] Polyacrylates **1** require long annealing times to observe phase transitions in the DSC and microscopic textures indicative of a liquid crystalline phase. Related 4′-(dialkylamino)-4-nitrostilbene side chain polyacrylates also have LC phases and are incompletely soluble, suggesting partial cross-linking during synthesis.[37] To improve the ability of the stilbene side chain polymers to order into liquid crystalline phases, we have prepared polysiloxanes **2** and **3** having donor–acceptor substituted stilbene mesogens.

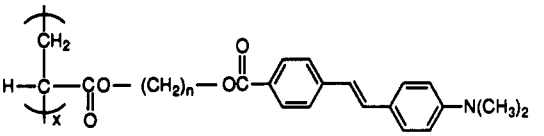

1; n = 2, 4, 6, 8, 10

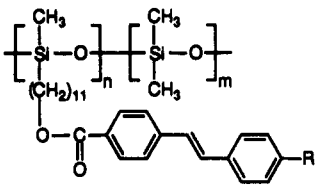

2a: R = —N(CH$_3$)$_2$ n = 60, m = 0

2b: n = 9, m = 8

3a: R = —N—O(CH$_2$)$_5$CH$_3$ n = 60, m = 0

3b: n = 9, m = 8

Experimental Section[38]

Materials. The poly(hydromethylsiloxane) (PHMS, Wacker, DP = 45–90) and poly(hydromethylsiloxane-*co*-dimethylsiloxane) (PHMS–PDMS, Petrarch, 50–55 wt % hydromethyl, M_n = 900–1000) were analyzed by ^{29}Si NMR spectroscopy and by size exclusion chromatography (SEC) in toluene solution with differential refractometer detection relative to polystyrene standards without universal calibration. The 79-MHz ^{29}Si NMR spectrum of PHMS–PDMS indicated a random copolymer, similar to that reported by Gray.[39] PHMS: SEC, M_n = 3800, M_w/M_n = 2.7; NMR, M_n = 3800, DP = 60 ± 3. PHMS–PDMS: SEC, M_n = 1050, M_w/M_n = 1.8; NMR, M_n = 1300, DP = 17 ■ 1, 9:8 HMS:DMS. All other reagents were obtained from Aldrich, analyzed by ^{1}H and ^{13}C NMR spectroscopy, and used as received. Melting points are uncorrected.

***N*-Acetyl-4-hydroxypiperidine (5).**[40] To a solution of 4-hydroxypiperidine (247 mmol, 25.0 g) and acetic anhydride (247

† Oklahoma State University.
‡ University of Florida.

0024-9297/93/2226-0659$04.00/0

mmol, 23.5 mL) was added an equivalent amount of anhydrous K_2CO_3, and the mixture was stirred at room temperature under dry air for 12 h. The product was extracted with CH_2Cl_2, and the solid K_2CO_3 was filtered off. The reaction mixture was not washed with water because the product is more soluble in water than in nonpolar organic solvents. White, hygroscopic crystals of **5** were collected by distillation at 130 °C and 0.25 mmHg: 28.47 g (81%). ^{1}H NMR ($CDCl_3$) δ 1.52 and 1.87 (2 m, 4 H, CH_2), 2.09 (s, 3 H, CH_3C=O), 3.21, 3.72, and 4.04 (3 m, 4 H, NCH_2), 3.90 (m, 1 H, OCH), 4.31 (s, 1 H, OH). ^{13}C NMR ($CDCl_3$) δ 21.2 (CH_3C=O), 33.5 (CH_2), 34.2 (CH_2), 38.8 (NCH_2), 43.6 (NCH_2), 66.2 (OCH), 168.9 (C=O). IR (neat, cm^{-1}) 3060–3700 (OH), 1630 (C=O). Anal. Calcd for $C_7H_{13}NO_2$: C, 58.72; H, 9.15; N, 9.78. Found: C, 58.67; H, 9.37; N, 9.68.

***N*-Acetyl-4-(hexyloxy)piperidine (6).** To a stirred slurry of 2.64 g (88 mmol) of NaH in 20 mL of dry *N*,*N*-dimethylformamide (DMF) were added under nitrogen 80 mmol (11.45 g) of **5** (dried at 25 °C under vacuum) and 5 mmol (1 mL) of 15-crown-5 ether. The mixture was stirred at room temperature for 15 min, and 1-bromohexane (80 mmol, 11.25 mL) was added. After 48 h at 25 °C, the mixture was poured into 150 mL of ice water, and the product was extracted with ether. The combined extracts were washed with H_2O, dried, and distilled at 120 °C and 0.25 mmHg to give 7.46 g (41%) of colorless liquid **6**. ^{1}H NMR ($CDCl_3$) δ 0.90 (t, 3 H, CH_3), 1.31 (m, 6 H, CH_2), 1.57 (m, 4 H, OCH_2CH_2 and $OCHCH_2$), 1.83 (m, 2 H, $OCHCH_2$), 2.09 (s, 3 H, CH_3C=O), 3.27, 3.65, and 3.90 (3 m, 4 H, NCH_2), 3.47 (overlapping t and m, 3 H, OCH and OCH_2). ^{13}C NMR ($CDCl_3$) δ 14.1 (CH_3), 21.5 (CH_3C=O), 22.6 (CH_3CH_2), 25.9 ($(CH_2)_2CH_2$), 30.0 (OCH_2CH_2), 30.6 ($OCHCH_2$), 31.7 ($CH_3CH_2CH_2$ and $OCHCH_2$), 38.8 (NCH_2), 43.7 (NCH_2), 68.2 (OCH_2), 73.8 (OCH), 168.8 (C=O). IR (neat, cm^{-1}) 1650 (C=O). Anal. Calcd for $C_{13}H_{25}NO_2$: C, 68.68; H, 11.08; N, 6.16. Found: C, 69.36; H, 10.69; N, 6.04.

4-(Hexyloxy)piperidine (7). A mixture of amide **6** (30 mmol, 6.82 g) and 3.5 M H_2SO_4 (300 mmol, 86 mL) was refluxed overnight. The mixture was poured into 150 mL of ice water, made basic with NaOH pellets, and extracted with diethyl ether. The dried extract was distilled at 80 °C and 0.25 mmHg to give 4.68 g (84%) of colorless liquid **7**. ^{1}H NMR ($CDCl_3$) δ 1.41 and 1.91 (2 m, 4 H, $OCHCH_2$), 1.54 (s, 1 H, NH), 1.56 (quintet, 2 H, J = 7 Hz, OCH_2CH_2), 2.60 and 3.08 (2 m, 4 H, NCH_2), 3.32 (m, 1 H, OCH), 3.44 (t, 2 H, J = 7 Hz, OCH_2). ^{13}C NMR ($CDCl_3$) δ 31.7 ($CH_3CH_2CH_2$), 33.2 ($OCHCH_2$), 44.7 (NCH_2), 67.8 (OCH_2), 75.6 (OCH). IR (neat, cm^{-1}) 3280 (NH). Anal. Calcd for $C_{11}H_{23}NO$: C, 71.30; H, 12.51; N, 7.56. Found: C, 70.89; H, 12.23; N, 7.59.

4-[4-(Hexyloxy)-1-piperidino]benzaldehyde (9). A mixture of compound **7** (27.8 mmol, 5.15 g), 4-fluorobenzaldehyde (27.8 mmol, 3.45 g), and 3.84 g of anhydrous K_2CO_3 in 5 mL of DMSO was stirred and heated under N_2 at 90 °C for 48 h. The mixture was poured into 250 mL of H_2O, and the precipitate was filtered. A white feather-like solid **9** was obtained after several recrystallizations from ethanol–water: 5.88 g (73%), mp 42–44 °C. ^{1}H NMR ($CDCl_3$) δ 1.70 and 1.94 (2 m, 4 H, $OCHCH_2$), 3.21 and 3.70 (2 m, 4 H, NCH_2), 3.47 (t, 2 H, J = 7 Hz, OCH_2), 3.61 (m, 1 H, OCH), 6.91 (d, 2 H, J = 9 Hz, Ar H3 and H5), 7.73 (d, 2 H, J = 9 Hz, Ar H2 and H6), 9.76 (s, 1 H, HC=O). ^{13}C NMR ($CDCl_3$) δ 30.6 ($OCHCH_2$), 44.9 (NCH_2), 68.2 (OCH_2), 73.9 (OCH), 113.4 (Ar C3 and C5), 126.5 (Ar C1), 132.0 (Ar C2 and C6), 154.8 (Ar C4), 190.3 (C=O). IR (KBr, cm^{-1}) 1680 (C=O), 1620 (C=C). UV–vis ($CHCl_3$) λ_{max} = 338 nm ($\epsilon = 2.79 \times 10^4$ M^{-1} cm^{-1}). Anal. Calcd for $C_{18}H_{27}NO_2$: C, 74.70; H, 9.40; N, 4.84. Found: C, 74.98; H, 9.62; N, 4.86.

4-[4-(Hexyloxy)-1-piperidino]-4′-carbomethoxy-*trans*-stilbene (11) was prepared by the procedure for 4-(dimethylamino)-4′-carbomethoxy-*trans*-stilbene (**10**),[35] using a solution of **9** (20 mmol, 5.79 g) and diethyl [4-(methoxycarbonyl)benzyl]phosphonate[35] (20 mmol, 5.72 g) in 30 mL of THF. After recrystallization from DMF, 7.07 g (84%) of greenish yellow powder **11** was obtained. DSC: C 178 °C M_1 227 °C M_2 252 °C I. No microscopic texture of mesophase M_1 or M_2 was observed due to decomposition at the isotropization temperature. ^{1}H NMR ($CDCl_3$) δ 1.71 and 1.97 (2 m, 4 H, $OCHCH_2$), 2.99 and 3.59 (2 m, 4 H, NCH_2), 3.47 (overlapping t and m, 3 H, J = 7 Hz, OCH and OCH_2), 3.91 (s, 3 H, CO_2CH_3), 6.91 (d, 2 H, J = 8.4 Hz, Ar H3 and H5), 6.95 (d, 1 H, J = 16.5 Hz, =$CHArCO_2R$), 7.12 (d, 1 H, J = 16.5 Hz, =$CHArNR_2$), 7.42 (d, 2 H, J = 8.4 Hz, Ar H2 and H6), 7.51 (d, 2 H, J = 8.2 Hz, Ar H2′ and H6′), 7.99 (d, 2 H, J = 8.2 Hz, Ar H3′ and H5′). ^{13}C NMR ($CDCl_3$) δ 30.9 ($OCHCH_2$), 46.6 (NCH_2), 52.0 (CO_2CH_3), 68.1 (OCH_2), 74.4 (OCH), 115.8 (Ar C3 and C5), 124.2 (=$CHArCO_2R$), 125.8 (Ar C2′ and C6′), 127.3 (Ar C1), 127.9 (Ar C2 and C6), 128.1 (Ar C4′), 129.9 (Ar C3′ and C5′), 131.1 (=$CHArNR_2$), 142.6 (Ar C1′), 151.1 (Ar C4), 167.0 (C=O). IR (KBr, cm^{-1}) 1720 (C=O), 1600 (C=C). UV–vis ($CHCl_3$) λ_{max} = 370 nm ($\epsilon = 3.38 \times 10^4$ M^{-1} cm^{-1}). Anal. Calcd for $C_{27}H_{35}NO_3$: C, 76.92; H, 8.37; N, 3.32. Found: C, 76.80; H, 8.42; N, 3.31.

10-Undecen-1-yl 4-(Dimethylamino)-*trans*-stilbene-4′-carboxylate (12). A mixture of 5.0 mmol (1.41 g) of compound **10**, 25 mmol (5 mL) of 10-undecen-1-ol, 1.0 mmol (0.27 g) of nickel acetylacetonate hydrate,[41] and 20 mL of xylene was refluxed in the dark for 92 h, after which compound **10** could no longer be detected by TLC using 15% ethyl acetate in hexane as eluant. Vigorous refluxing was needed to drive off the methanol formed. The black solid was filtered and washed with ethyl acetate. The filtrate was washed with H_2O and dried. The crude product was recrystallized from ethanol to give a greenish yellow powder: 1.39 g (66%). ^{1}H NMR ($CDCl_3$) δ 1.37 (m, 12 H, $(CH_2)_6$), 1.76 (quintet, 2 H, J = 7 Hz, $CO_2CH_2CH_2$), 2.04 (q, 2 H, J = 7 Hz, =$CHCH_2$), 2.99 (s, 6 H, NCH_3), 4.30 (t, 2 H, J = 7 Hz, CO_2CH_2), 4.97 (m, 2 H, =CH_2), 5.80 (m, 1 H, =CH), 6.71 (d, 2 H, J = 8.8 Hz, Ar H3 and H5), 6.92 (d, 1 H, J = 16.2 Hz, =$CHArCO_2R$), 7.15 (d, 1 H, J = 16.3 Hz, =$CHArNR_2$), 7.43 (d, 2 H, J = 8.8 Hz, Ar H2 and H6), 7.51 (d, 2 H, J = 8.4 Hz, Ar H2′ and H6′), 7.98 (d, 2 H, J = 8.3 Hz, Ar H3′ and H5′). ^{13}C NMR ($CDCl_3$) δ 25.9, 28.6, 28.8, 29.0, 29.1, 29.2, and 29.3 ($(CH)_7$) 33.6 (=$CHCH_2$), 40.2 (NCH_3), 64.8 (CO_2CH_2), 112.1 (Ar C3 and C5), 114.0 (=CH_2), 122.9 (=$CHArCO_2R$), 124.9 (Ar C1), 125.5 (Ar C2′ and C6′), 127.8 (Ar C2 and C6), 128.1 (Ar C4′), 129.8 (Ar C3′ and C5′), 131.2 (=$CHArNR_2$), 139.1 (=CH), 142.6 (Ar C1′), 150.3 (Ar C4), 166.5 (C=O). IR (KBr, cm^{-1}) 1710 (C=O), 1600 (C=C). UV–vis ($CHCl_3$) λ_{max} = 381 nm ($\epsilon = 3.05 \times 10^4$ M^{-1} cm^{-1}). Anal. Calcd for $C_{28}H_{37}NO_2$: C, 80.15; H, 8.89; N, 3.34. Found: C, 80.52; H, 8.97; N, 3.31.

10-Undecen-1-yl 4-[4-(Hexyloxy)-1-piperidino]-*trans*-stilbene-4′-carboxylate (13). The procedure for **12** was followed using 5.0 mmol (2.10 g) of compound **11**. Recrystallization from ethanol gave 1.94 g (69%) of greenish yellow powder **13**. ^{1}H NMR ($CDCl_3$) δ 1.37 (m, 18 H, $(CH_2)_6$ and $(CH_2)_3CH_3$), 1.73 (m, 4 H, $CO_2CH_2CH_2$ and $OCHCH_2$), 2.02 (m, 4 H, =$CHCH_2$ and $OCHCH_2$), 4.30 (t, 2 H, J = 7 Hz, CO_2CH_2), 4.97 (m, 2 H, =CH_2), 5.80 (m, 1 H, =CH). ^{13}C NMR ($CDCl_3$) δ 26.0, 28.7, 28.9, 29.1, 29.2, 29.4 and 29.5 ($(CH_2)_7$), 33.8 (=$CHCH_2$), 65.0 (CO_2CH_2), 114.1 (=CH_2), 139.2 (=CH). IR (KBr, cm^{-1}) 1710 (C=O), 1600 (C=C). UV–vis ($CHCl_3$) λ_{max} = 369 nm ($\epsilon = 2.97 \times 10^4$ M^{-1} cm^{-1}). Anal. Calcd for $C_{37}H_{53}NO_3$: C, 79.38; H, 9.54; N, 2.50. Found: C, 78.86; H, 9.76; N, 2.42.

Hydrosilylation. The starting polysiloxane and a 10 mol % excess of the appropriate undecenyl ester **12** or **13** (with respect to the Si–H bonds) were dissolved in 30 mL of dry toluene (freshly distilled and dried over molecular sieves). A freshly prepared equimolar solution of chloroplatinic acid (H_2PtCl_6)[42] and triethylamine in 2-propanol was added to give a Pt:alkene ratio of 10^{-4}. The triethylamine neutralizes the HCl, which otherwise would protonate the amino group of the monomers. The mixture was kept in the dark at 100 °C for about 48 h under Ar until negligible Si–H absorption (2160 cm^{-1}) was detectable by IR spectroscopy. An amount of 1-octene equimolar to the original Si–H was added. After 24 h at 100 °C, the polymer was precipitated by addition of methanol. Polymers **2b**, **3a**, and **3b** (2 g) were reprecipitated from 30 mL of chloroform solution by slow addition of 300 mL of methanol with continuous stirring, and filtered through a fine-porosity fritted funnel. Each polymer was precipitated 6–7 times, and purity was checked by SEC. The ^{29}Si NMR spectra of the final side chain polysiloxanes showed no peaks at −37 ppm for the Si–H groups. However, ^{1}H NMR spectra indicated <100% conversion by a small peak at 4.7 ppm for Si–H groups. Best fits of structures to the elemental analyses are reported in Table I. Comparison to theoretical analyses of products of 100% yield are in the following paragraphs.

Table I
Analyses of Side Chain Polysiloxanes by ^{1}H NMR and Elemental Analysis

	% conversion of SiH		% octyl side chain		% mesogen side chain	
polymer	NMR	EA	NMR	EA	NMR	EA
2a	91	96	12	29	79	67
2b	93	100	10	11	83	89
3a	94	85	*a*	27	*a*	58
3b	93	100	*a*	11	*a*	89

[a] Not analyzed because of overlapping CH_3 peaks.

Polymer 2a. A mixture of 0.41 g (6.5 mmol (Si–H)) of PHMS and 3.00 g (7.15 mmol) of **12** was used. Polymer **2a** was fractionated by dissolving 2.5 g in about 25 mL of hot toluene, filtering quickly through fluted filter paper, cooling to room temperature, and then cooling in an ice bath. The polymer was vacuum filtered through a fine-porosity fritted funnel. After precipitations, 2.15 g (69%) of greenish yellow powder was obtained. The NMR spectra of **2a** were like those of **12** except that scalar couplings were not observed due to broad peaks. ^{1}H NMR ($CDCl_3$) δ 0.04 (Si–CH_3), 0.12 (terminal Si–CH_3), 0.49 (Si–CH_2), 0.84 (CH_3), 1.32 ((CH_2)$_6$ and (CH_2)$_8$). ^{13}C NMR ($CDCl_3$) δ 17.7 (Si–CH_2), 23.1, 26.1, 28.8, 29.5, 29.6, 29.7, 29.8, 32.0, and 33.6 ((CH_2)$_6$ and (CH_2)$_9$). ^{29}Si NMR ($CDCl_3$) δ −21.3 to −22.9 (CH_3–Si–CH_2). IR (KBr, cm^{-1}) 2150 (small peak, Si–H), 1710 (C=O), 1600 (C=C), 1100–1010 (Si–O). UV-vis ($CHCl_3$) λ_{max} = 382 nm. Anal. Calcd for pure **2a**: C, 72.45; H, 8.63; N, 2.90; Si, 6.02. Found: C, 71.32; H, 9.69; N, 2.12; Si, 7.87.

Polymer 2b. The general procedure was followed using 0.93 g (6.5 mmol (Si–H)) of PHMS–PDMS. After precipitations, 2.29 g (63%) of greenish yellow powder was obtained. ^{1}H NMR ($CDCl_3$) δ 0.04 (Si–CH_3), 0.12 (terminal Si–CH_3), 0.48 (Si–CH_2), 0.85 (CH_3), 1.25 ((CH_2)$_6$ and (CH_2)$_8$). ^{13}C NMR ($CDCl_3$) δ 1.1 (Si–CH_3), 1.2 (terminal Si–CH_3), 17.6 (Si–CH_2), 23.1, 26.1, 28.8, 29.4, 29.5, 29.7, 32.0, and 33.5 ((CH_2)$_6$ and (CH_2)$_9$). ^{29}Si NMR ($CDCl_3$) δ −21.8 to −23.0 (CH_3–Si–CH_2 and CH_3–Si–CH_3), 6.8, 6.9, 7.1, and 7.2 (terminal Si). IR (KBr, cm^{-1}) 2150 (small peak, Si–H), 1710 (C=O), 1600 (C=C), 1100–1010 (Si–O). UV-vis ($CHCl_3$) λ_{max} = 382 nm. Anal. Calcd for pure **2b**: C, 67.00; H, 8.64; N, 2.48; Si, 10.52. Found: C, 66.05; H, 8.45; N, 2.30; Si, 10.39.

Polymer 3a. The general procedure was followed using a mixture of 0.25 g (4.0 mmol (Si–H)) of poly(hydromethylsiloxane) and 2.50 g (4.47 mmol) of **13**. After precipitations, 1.38 g (55%) of greenish yellow powder was obtained. ^{1}H NMR ($CDCl_3$) δ 0.05 (Si–CH_3), 0.51 (Si–CH_2), 1.29 ((CH_2)$_3$, (CH_2)$_6$, and (CH_2)$_8$). ^{13}C NMR ($CDCl_3$) δ 17.7 (Si–CH_2), 23.1, 25.9, 26.1, 28.8, 29.5, 29.7, 29.8, 30.1, 30.2, and 33.6 ((CH_2)$_2$, (CH_2)$_6$, and (CH_2)$_9$). ^{29}Si NMR ($CDCl_3$) δ −21.4 to −23.2 (CH_3–Si–CH_2), 6.7 (terminal Si). IR (KBr, cm^{-1}) 2150 (small peak, Si–H), 1710 (C=O), 1600 (C=C), 1110–1010 (Si–O). UV-vis ($CHCl_3$) λ_{max} = 371 nm. Anal. Calcd for pure **3a**: C, 73.48; H, 9.28; N, 2.25; Si, 4.66. Found: C, 70.02; H, 9.04; N, 1.66; Si, 7.59.

Polymer 3b. The general procedure was followed using 0.58 g (4.0 mmol (Si–H)) of PHMS–PDMS. After precipitations, 1.70 g (60%) of greenish yellow powder was obtained. ^{1}H NMR ($CDCl_3$) δ 0.04 (Si–CH_3), 0.49 (Si–CH_2), 1.30 ((CH_2)$_3$, (CH_2)$_6$, and (CH_2)$_8$). ^{13}C NMR ($CDCl_3$) δ 1.2 (Si–CH_3), 1.9 (terminal Si–CH_3), 17.6 (Si–CH_2), 23.1, 25.9, 26.1, 28.8, 29.4, 29.7, 30.1, 30.2, and 33.5 ((CH_2)$_2$, (CH_2)$_6$, and (CH_2)$_9$). ^{29}Si NMR ($CDCl_3$) δ −21.8 to −22.9 (CH_3–Si–CH_2 and CH_3–Si–CH_3), 6.8, 6.9, 7.1, and 7.2 (terminal Si). IR (KBr, cm^{-1}) 2140 (small peak, Si–H), 1710 (C=O), 1600 (C=C), 1110–1010 (Si–H). UV-vis ($CHCl_3$) λ_{max} = 369 nm. Anal. Calcd for pure **3b**: C, 69.01; H, 9.21; N, 1.99; Si, 8.42. Found: C, 67.65; H, 9.09; N, 1.64; Si, 9.12.

Measurements. SEC analyses of SCLCPs were performed at 25 °C using three polystyrene gel columns of 10^2, 10^3 and 10^4 Å obtained from Polymer Laboratories, Ltd., solutions of 10 mg of polymer/mL of THF, a flow rate of 1 mL/min, UV detection, and polystyrene standards of M_n = (0.8–600) × 10^3 using cubic fit values. Differential scanning calorimetry (DSC) measurements were performed with a Perkin-Elmer DSC-2 instrument equipped with a TADS 3600 data station. Two separate 20 K/min scans were done for each polymer: −123 to +77 °C with helium as purge gas for the sample enclosure and 37 to about 250 °C, using nitrogen as purge gas and indium calibration. Glass transition temperatures (T_g) were read at the midpoint of the change in the heat capacity. The phase transition temperatures and mesomorphic textures were observed with a Nikon OPTIPHOT-POL microscope with crossed polarizers and equipped with a Mettler FP82 hot stage controlled by a Mettler FP80 thermoregulator. Observations were made at rates between 10 and 1 K/min, and transition temperatures quoted are from extrapolation to zero rate. The polymers were viscous in the mesophases, and annealing at elevated temperatures for several hours was necessary to obtain good textures. X-ray powder diffraction measurements were performed with Cu Kα radiation, using a Philips APD 3720 high-temperature X-ray diffractometer equipped with a tantalum heating plate controlled by a thermoregulator. The sample chamber was purged with helium during each measurement. The samples were heated above the clearing point to erase any previous thermal history and then cooled to the desired temperatures for measurement.

Langmuir–Blodgett (LB) measurements were performed with a KSV Instruments Model 5000 trough equipped with one barrier for unsymmetrical compression and both floating barrier and Wilhelmy plate surface pressure sensors. Monolayers were spread on the water subphase from chloroform solutions (0.5 mg/mL) at 27–30 °C and were compressed at barrier speeds of 25 to 5 mm/min. Octadecyltrichlorosilane-treated quartz slides (25 × 25 × 2 mm) were used for transfer experiments. Monolayers were spread on the water subphase and were symmetrically compressed using two barriers at a speed of 5 mm/min. Monolayer transfer was carried out at a constant surface pressure of 20 mN/m and barrier speed of 1.0 mm/min after allowing 30 min for the monolayers to stabilize. The substrate transfer speed was 1.0 mm/min.

Results

Synthesis. 4-[4-(Hexyloxy)-1-piperidino]benzaldehyde (**9**) and the monomers **12** and **13** were synthesized as shown in Scheme I. The ^{1}H NMR spectra of all stilbene compounds and polymers showed that only the trans isomer was present. The (hexyloxy)piperidino compounds **11** and **13** and polymers **3a** and **3b** are much more soluble than the dimethylamino analogues in solvents such as $CHCl_3$. Scheme II illustrates the hydrosilylation of the monomers **12** and **13** with either poly(hydromethylsiloxane) or the copolymer of 50% hydromethylsiloxane–50% dimethylsiloxane, with hexachloroplatinic acid as the catalyst. Several attempts at hydrosilylation of **12** using (divinyltetramethyldisiloxane)platinum[43–45] catalyst with either the homo- or the copolysiloxane gave yellow precipitates that were insoluble in all organic solvents including chloroform, indicative of cross-linked polymers.

The contents of unreacted Si–H groups of all four polymers and of octyl side chains of **2a** and **2b** were measured from ^{1}H NMR spectra. However, the CH_3 signal of the octyl chain is superposed with the methyl signal of the hexyl group for **3a** and **3b**. The percent conversion and the octyl side chain content were also estimated from the elemental analyses reported in Table I.

Each polymer was reprecipitated 6 or 7 times to remove residual monomer **12** or **13**. The M_n values based on the DP of the starting polysiloxanes and degrees of substitution of SCLCPs from NMR spectra are in Table II. SEC analyses of the molecular weights based on polystyrene standards and residual monomer contents of the final polysiloxanes are also in Table II. The purified polymers have polydispersity indices, M_w/M_n, ranging from 1.4 to 1.9, lower than those of the starting polysiloxanes due to the fractionation of oligomers. SEC analyses using polystyrene standards underestimate the molecular weights of SCLCPs because the hydrodynamic volume of a

Scheme I

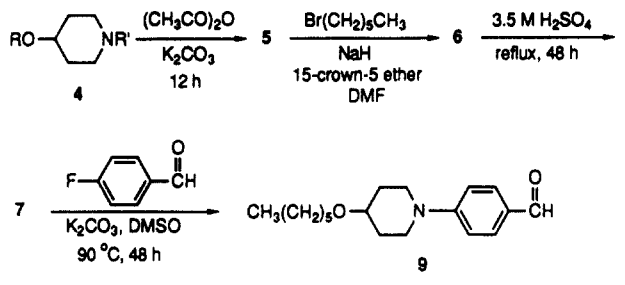

4: R = R' = H
5: R = H, R' = $COCH_3$
6: R = $CH_3(CH_2)_5$, R' = $COCH_3$
7: R = $CH_3(CH_2)_5$, R' = H

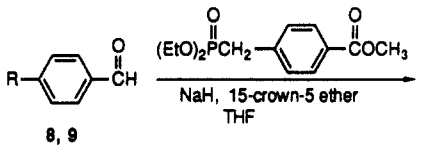

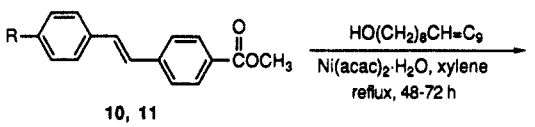

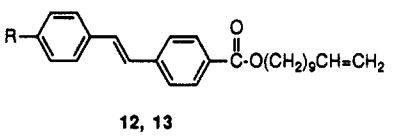

8, 10, 12: R = —$N(CH_3)_2$

9, 11, 13: R = —N—$O(CH_2)_5CH_3$

Scheme II

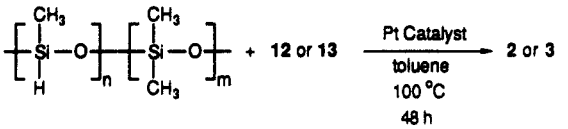

Table II
Analyses of Side Chain Polysiloxanes

	SEC		NMR	elem anal.	
polymer	M_n	M_w	M_n	M_n	% monomer
2a	6800	9800	24500	19900	<1
2b	5400	8800	4500	4300	<1
3a	19400	37600	32100	22700	2
3b	7200	10500	5600	5400	5

comblike polymer is smaller than that of polystyrene of the same molecular weight.[46]

Liquid Crystal Phases. Phase transitions of the precursor undecenyl stilbenecarboxylates and the polysiloxanes measured by DSC and microscopy are summarized in Table III.[38] The phase assignments are based on powder X-ray diffraction and polarizing microscopy. The isotropization temperatures of all of the side chain polysiloxanes were obtained by microscopy, because the heats of transition from the mesophase to the isotropic liquid phase were too small to observe by DSC.

Two highly ordered mesophases of (hexyloxy)piperidinostilbene **13** were observed by thermal analysis, while only a melting transition was observed for (dimethylamino)stilbene **12**. The (hexyloxy)piperidino group both lengthens the mesogen and makes it more flexible, thus giving it a wider range of liquid crystalline properties. The powder X-ray diffraction pattern of the high-temperature phase of **13** shows a sharp peak in the small-angle region and a diffuse peak in the wide-angle region, characteristic of smectic A or C phases. The X-ray pattern at 165 °C, attributed to a smectic B phase, exhibits a sharp peak in the wide-angle region in addition to the sharp peaks in the small-angle region. This outer reflection corresponds to 110 and 200 reflections, which indicate order within the smectic layers. [(Hexyloxy)piperidino]stilbene **13** exhibited the distinctive simple focal conic texture of a smectic A phase at 177 °C. Three peaks in the wide-angle region of the X-ray pattern of the powderlike sample of (dimethylamino)stilbene **12** at 135 °C indicate a well-ordered structure in which the molecular long axes are orthogonal to layer planes. At first, this phase was thought to be a smectic E phase.[47] However, the texture suggests an orthorhombic crystalline structure.

There was no evidence of any glass transition for homopolysiloxane **2a** by DSC in the range from −123 to +146 °C. This might be due to the small volume fraction of the siloxane backbone compared to the side chain mesogen, making the glass transition too weak to detect. Due to the high viscosity of the polymer, broad peaks are observed in DSC scans. Figure 1 shows thermograms of **2a**. Only one mesophase was assigned for **2a**, although there are three overlapping peaks at about 167–195 °C, which may be due to more mesophases. There was no significant change in the phase transition temperatures and no resolution of the overlapping peaks at different scan rates. The thermogram of a mixture containing 90 wt % **2a** and 10 wt % **12** was investigated to determine the effect of residual monomer in the polymer sample. The phase transition temperature range and peaks recorded were almost the same as those of "pure" **2a**. Annealing at 190 °C for hours was needed to give a fiberlike texture of **2a**, typical of high molecular weight smectic polymers. Since **2a** was birefringent at 210 °C, the diffuse powder X-ray diffraction pattern indicated a nematic phase.

[(Hexyloxy)piperidino]stilbene homopolysiloxane **3a** has both a high-temperature nematic phase and an ordered phase (Figure 2) that might be S_B from the powder X-ray diffraction pattern at 120 °C, except for an absence of reflections in the small-angle region (Figure 3), which means the absence of layers. Possibly this mesophase is an ordered nematic with hexagonal structure rather than smectic B. Friedzon and co-workers[48] reported a similar X-ray pattern and suggested that it was due to a new phase, N_B, in which the mesogenic groups were packed in a hexagonal array but without translational order in the direction of their long axes. As for **2a**, no microscopic texture was obtained for **3a**.

Copolysiloxanes **2b** and **3b** have similar weak, wide glass transitions near −40 °C. Both have several DSC peaks in the region of the transition to the S_A phase, shown in Figures 4 and 5. There was no significant change in the thermograms with varying scan rates. Copolymer **2b** has a fine-grained texture at 170 °C in the S_A phase. In addition to the observed high-temperature S_A phase, which was assigned from the X-ray diffraction at 205 °C, a low-temperature mesophase was observed for **3b** and assigned an S_B structure. The powder X-ray diffraction pattern at 171 °C showed the typical sharp peaks in the small-angle region denoting the presence of layers and a strong sharp peak in the wide-angle region which corresponds to 110 and 200 reflections. Figure 6 shows a typical fan-shaped texture of an S_A phase of **3b**.

Table III
Phase Transition Temperatures of Monomers and Polysiloxanes

sample	phase transition temperature,[a] °C (ΔH, kcal/mol of mesogen)									
12			C	146	I					
2a			C	167–195 (4.84)	N	215[b]	I			
2b	G	−35	C	146–178 (7.06)	S_A	183[b]	I			
13			C	109 (0.54)	S_B	172 (1.52)	S_A	183	I	
3a			C	110–118 (0.15)	S_B[c]	192–211 (1.0)	N	258[b]	I	
3b	G	−43	C	112–126 (0.27)	S_B	182–197 (1.04)	S_A	220[b]	I	

[a] C = orthorhombic crystal or smectic E, I = isotropic liquid, N = nematic, G = glass, S_A = smectic A, S_B = smectic B. [b] Transition temperatures were determined by microscopy. All other data are from DSC. [c] Possibly an ordered nematic.

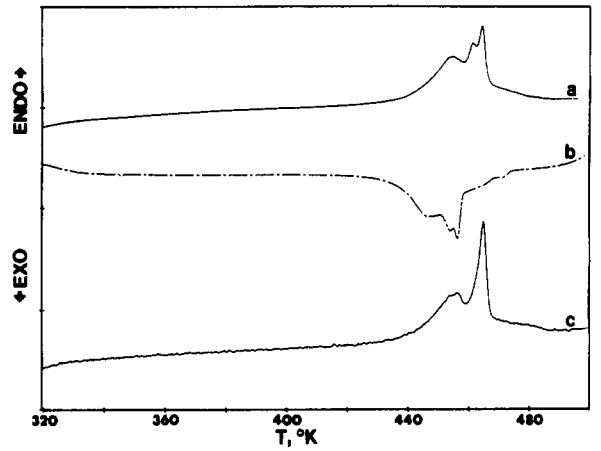

Figure 1. DSC analyses of **2a** at 20 K/min: (a) second heating scan; (b) cooling scan; (c) with 10% residual monomer **12**.

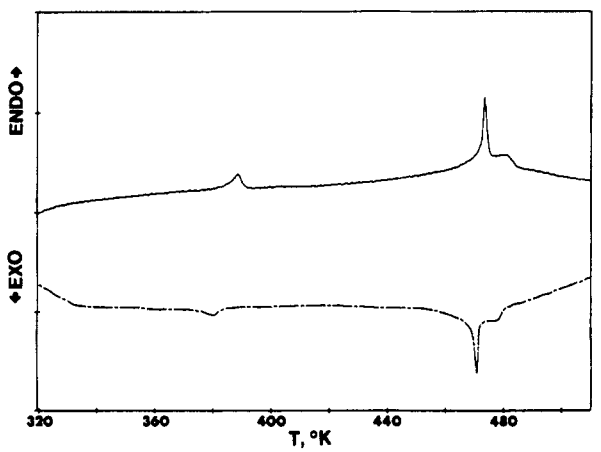

Figure 2. DSC thermograms of **3a** at 20 K/min; second heating and cooling scans.

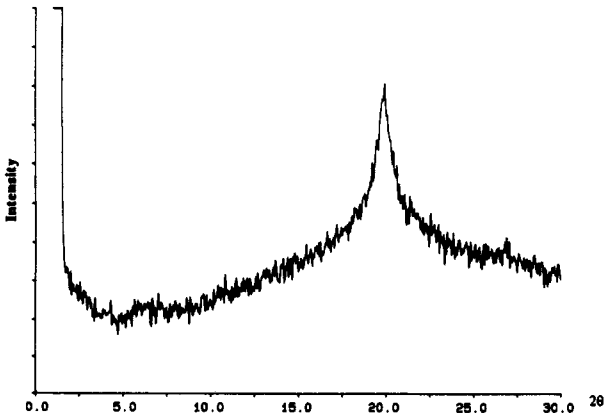

Figure 3. Powder X-ray diffraction pattern of **3a** at 120 °C.

All of the polysiloxanes exhibited a low-temperature crystalline phase identified by X-ray diffraction patterns and reported in Table III. Figure 7 shows a sample X-ray pattern of this phase of **2a** at 150 °C. The three sharp

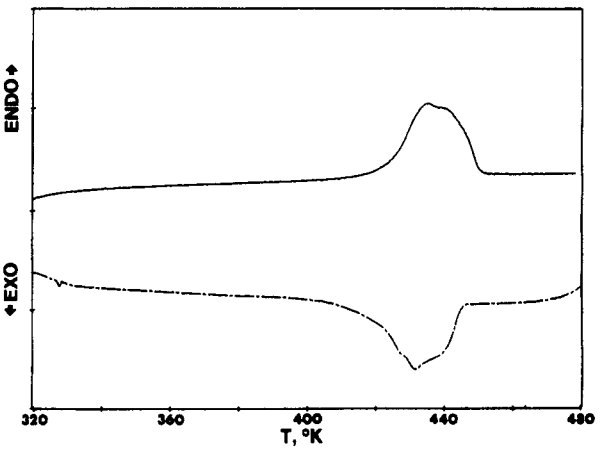

Figure 4. DSC thermograms of **2b** at 20 K/min; second heating and cooling scans.

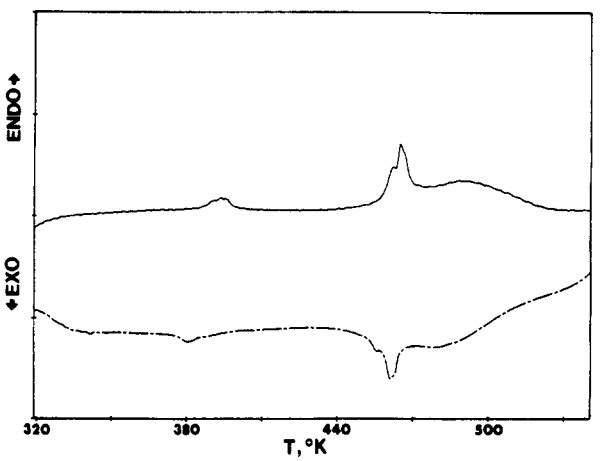

Figure 5. DSC thermograms of **3b** at 20 K/min; second heating and cooling scans.

peaks in the wide-angle region corresponding to 110, 200, and 210 reflections are characteristic of an orthorhombic crystal. Sharp peaks in the small-angle region indicate a layered phase. This might possibly be an S_E phase, which also gives three reflections in the wide-angle region. X-ray diffraction studies on oriented samples would be needed to distinguish these possibilities.

The X-ray data of the monomers and polysiloxanes are reported in Tables IV and V. The length of the most stable conformation of each mesogen was calculated by a computer molecular modeling program (PCMODEL, Version 4.3) for comparison with the *d* spacings.

Monolayers. The monolayers of the polysiloxanes were characterized by room temperature measurement of the film pressure (Π) vs mean molecular area (Mma) isotherms, shown in Figure 8. In this work, mean molecular area is defined as area per mesogenic repeat unit of the polysiloxane. The isotherms of **2a** and **2b** have no observable discontinuities and show no evidence of phase transformations. Extrapolation of the steeply sloping linear region

Figure 6. Fanlike texture between crossed polarizers of **3b** after overnight annealing at 175 °C.

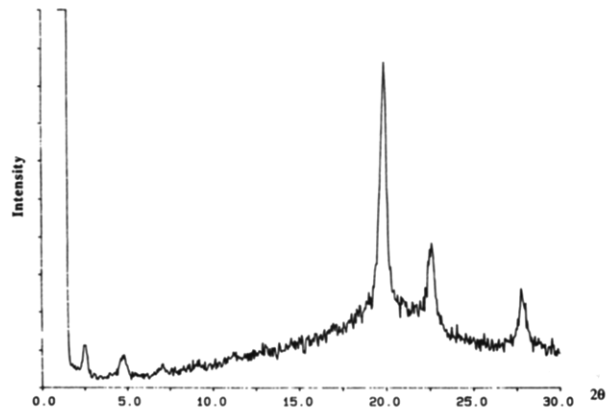

Figure 7. Powder X-ray diffraction pattern of **2a** at 150 °C, illustrating an orthorhombic crystalline structure.

to zero surface pressure gives the area per repeat unit of closely packed monolayers of ~23 and ~34 Å^2 for **2a** and **2b**, respectively. The closely packed phases of **3a** and **3b** have mean repeat unit areas of ~30 Å^2. Because the side chain polysiloxane films exhibited high viscosities, it was necessary to use a Langmuir balance rather than a Wilhelmy plate to measure surface pressure. The films can be compressed to at least 50 mN/m with no apparent collapse. Only **2b** showed a possible collapse of the monolayer at about 53 mN/m, which alternatively could be just a rearrangement of the polymer chains or side chains. The copolysiloxanes **2b** and **3b** showed less hysteresis than the homopolysiloxanes **2a** and **3a** upon compression and subsequent expansion of the monolayers. Repeated compression–expansion runs of **2b** and **3b** have much improved hysteresis behavior. Figures 9 and 10 show that the isobaric Mma's decrease during the first 30 min and change much less over longer time. There were greater

Table IV
X-ray Diffusion Data of Monomers and Polysiloxanes

sample	temp, °C	*d* spacing, Å	(*hkl*)
12[a]	135 (crystal)	32.49	(001)
		16.49	(002)
		10.97	(003)
		8.28	(004)
		4.55	(110)
		3.99	(200)
		3.24	(210)
2a	210 (N)	4.87	
2b	180 (S_A)	37.44	(001)
		4.63	
13[b]	177 (S_A)	33.72	(001)
		18.26	(002)
		4.86	
	165 (S_B)	34.25	(001)
		18.72	(002)
		4.53	
3a	230 (N)	4.61	
	120 (S_B)	4.47	
3b	205 (S_A)	40.90	(001)
		21.87	(002)
		4.65	
	171 (S_B)	45.53	(001)
		24.54	(002)
		4.57	

[a] Calculated length ≈ 27.8 Å. [b] Calculated length ≈ 37.5 Å.

Table V
Crystal Data of Monomers and Polymers

		unit cell, Å				
sample	temp, °C	*a*	*b*	*c*	V,[a] Å^3	D_x,[a] g/cm
12	135	8.0	5.5	32.5	1430	0.97
2a	150	7.9	5.4	35.4	1510	1.06
2b	136	7.9	5.5	40.9	1777	1.02
13	30	8.2	5.4	38.1	1687	1.10
3a	30	8.2	5.4	45.1	1997	1.03
3b	30	8.2	5.5	50.2	2264	1.01

[a] V and D_x were calculated from the values of a, b, c, and $Z = 2$.

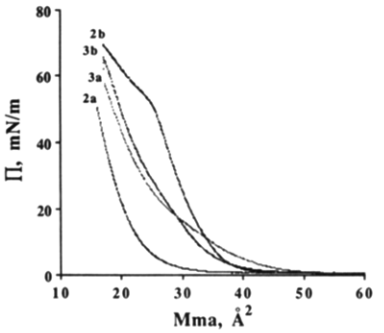

Figure 8. Surface pressure–area isotherms of polysiloxanes at room temperature.

decreases of the Mma with homopolymers **2a** and **3a** than with copolymers **2b** and **3b** and with the (hexyloxy)-piperidino side chain polymers **3a** and **3b** than with (dimethylamino)stilbene polymers **2a** and **2b**.

In preliminary experiments, the polysiloxanes were transferred onto hydrophobic, octadecyltrichlorosilane-treated quartz slides. Attempts at deposition onto a hydrophilic substrate failed. LB multilayers of **2b** were obtained with transfer ratios of 0.8 during the first downstroke, 0.3 during the first upstroke, and decreasing transfer ratios of 0.4–0.2 on succeeding downstrokes. Transfers were stopped after six partial layers. Monolayers of **3b** also transferred, although the transfer ratios of the first downstroke and the first upstroke were only 0.5 and 0.2, respectively. Transfers were stopped after four layers. Homopolymers **2a** and **3a** did not transfer. UV–vis spectra

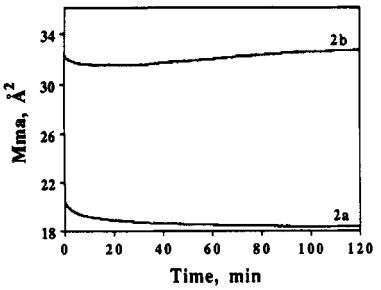

Figure 9. Isobaric creep measurements (15 mN/m) of (dimethylamino)stilbene polysiloxanes at room temperature.

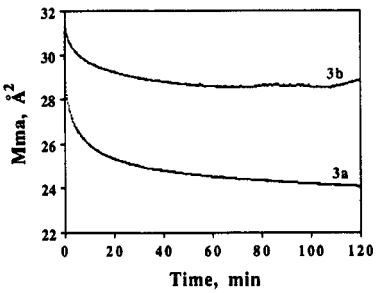

Figure 10. Isobaric creep measurements (15 mN/m) of [(hexyloxy)piperidino]stilbene polysiloxanes at room temperature.

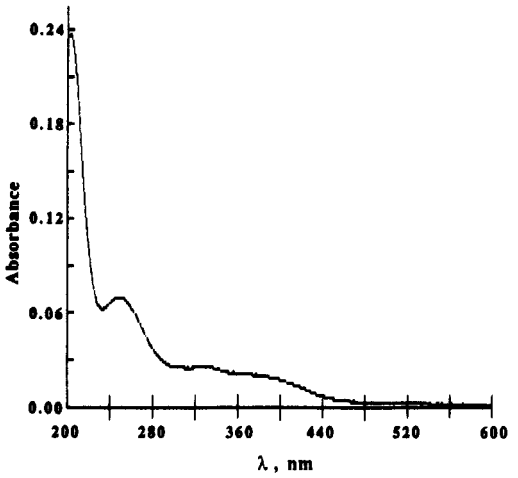

Figure 11. UV–vis spectrum of an LB film of **2b**.

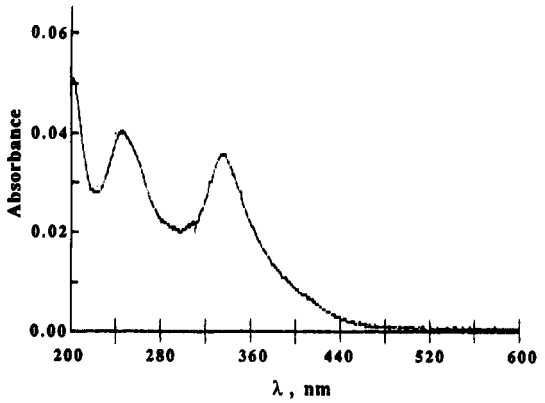

Figure 12. UV–vis spectrum of an LB film of **3b**.

of the transferred multilayers of **2b** and **3b** are shown in Figures 11 and 12. The addition of a small amount of monomer did not help stabilize the monolayers.

Discussion

Polymer Characterization. The phase transitions of SCLCPs are strongly influenced by molecular weight and molecular weight distribution. Side chain polysiloxanes contaminated with monomer show broad peaks and lower transition temperatures than the polymer alone by DSC.[49] Six or seven reprecipitations of the polymers did not remove all of the monomers **12** and **13** (Table II). Thus, the phase transition temperatures reported in Table III must be considered lower limits to the values that would be achieved in the absence of residual monomer.

The relative SEC molecular weights of the side chain homopolysiloxanes based on polystyrene standards, reported in Table II, are much lower than the true molecular weights from ^{1}H NMR end group analysis. For example, the starting poly(hydromethylsiloxane) used to prepare **2a** and **3a** has DP = 60 by ^{29}Si NMR analysis. After hydrosilylation with **12** and capping the remaining Si–H groups with 1-octene, ^{1}H NMR analysis of the mesogenic side chains, the unreacted Si–H groups, and the octyl side chains gives a calculated M_n = 24 500. Similarly, the best fit of mesogenic side chains, Si–H groups, and octyl side chains to elemental analyses gives M_n = 22 500. In contrast, by SEC analysis relative to polystyrene standards **2a** has M_n = 6800. Because of possible increases in DP due to fractionation of the SCLCPs, the true values of M_n may be even larger than the NMR values in Table II. Similarly, M_n of **3a** is 32 100 by ^{1}H NMR analysis or 25 200 by elemental analysis compared with 19 400 by SEC. The greater difference between the SEC and the direct measurements of M_n for **2a** than for **3a** may be due to lesser solvation of the (dimethylamino)stilbene than of the [(hexyloxy)piperidino]stilbene side chains in THF solution, giving a relatively smaller hydrodynamic volume of **2a**. There was little difference between the M_n values by ^{1}H NMR, elemental analysis, and SEC for copolysiloxanes **2b** and **3b**. Previously, Duran and Strazielle[46] showed that the weight-average molecular weights of a series of SCLC polymethacrylates measured by SEC calibrated with polystyrene standards were systematically lower than those obtained by light scattering by factors of 0.4–0.6, and Lang and Burchard[50] showed that for the same molecular weight, the elution volume is shifted to larger values as the average number of branches of polymethacrylates is increased (using linear PMMA as the reference polymer).

Molecular weights and molecular weight distributions of SCLCPs can influence the phases formed as well as the transition temperatures. SCLC poly(vinyl ether)s have different mesophases at different molecular weights in the range 1300–18 000.[51–53] SCLC poly(vinyl ether)s with cyanobiphenyl mesogens having DP from 1 to 30 and M_w/M_n of 1.1 showed a continuous change of the mesomorphic–isotropic phase transitions from nematic–isotropic to smectic–isotropic with increasing molecular weight.[54] The T_i of polysiloxanes with 4-substituted phenyl benzoate mesogens increased greatly up to DP ≤ 10 and only slightly at DP > 10; the T_g and the mesophase-to-mesophase transition temperatures (T_{1c}) also increased with increasing DP, but not as much as the corresponding T_i.[55] At DP > 10, T_g and T_{1c} remained nearly constant. Similarly, T_g and T_i of SCLC polysiloxanes with 4-cyanophenyl benzoate mesogens increased with increasing DP at approximately constant M_w/M_n values up to DP of 100; decrease of M_w/M_n from 1.9 to 1.25 increased T_g and T_i by approximately 5 °C.[56] From these earlier investigations, we conclude that the molecular weights of homopolymers **2a** and **3a** are sufficiently high that further increase of the degree of substitution of mesogens on the siloxane would have only minor effects on their transition temperatures. However, copolymers **2b** and **3b**, having DP = 17 and only half of the silicon atoms substituted with mesogenic side chains,

would likely have higher transition temperatures if they had higher molecular weights.

Liquid Crystal Phases. The appearance of a liquid crystalline phase when a mesogenic structure is incorporated into a flexible polymer is well known experimentally[22] and has a thermodynamic basis.[57] (Dimethylamino)stilbene **12** has no liquid crystalline phase but forms nematic homopolysiloxane **2a** and smectic A copolysiloxane **2b**. The greater flexibility of the copolymer allows a higher degree of order into layered phases. The high degree of substitution of mesogens in homopolysiloxane **2a** apparently does not allow much order even in the semicrystalline state, as evidenced by the small ΔH of melting into the nematic phase of **2a** compared with ΔH_m of **2b** into the S_A phase. Both **2a** and **2b** are slow to order into recognizable polarizing microscopic textures even after annealing for days at 5 °C below T_i, but they do give reproducible DSC thermograms at 20 K/min. Polyacrylates having the same mesogen require hours of annealing in the mesophase between scans to attain reproducible DSC heating curves.[35]

The third six-membered ring of the piperidinostilbene core and flexible tails at both ends of the mesogen cause [(hexyloxy)piperidino]stilbene **13**, homopolysiloxane **3a**, and copolysiloxane **3b** to have more ordered smectic phases than the corresponding (dimethylamino)stilbene compound and polymers. Increased mesophase order due to longer mesogen cores is well known.[58] Compound **13** and polymers **3a** and **3b** have smectic B phases. These phases are not smectic F or I, because dimorphism is known for the transformation of an S_B phase to an S_A phase with increasing temperature but not for transformation of an S_F or S_I phase to an S_A phase. The mesogenic groups in both S_A and S_B phases are oriented normal to the smectic layers. On the other hand, when tilted S_F and S_I phases are present, the sequence of liquid crystalline phases is S_F S_I S_C, and S_A, if present. Trimorphism having the sequence S_E S_B S_A is also possible.[59] The C–S_B transition temperatures of the (hexyloxy)piperidino polymers **3a** and **3b** are lower than the C–N or S_A transition temperatures of dimethylamino polymers **2a** and **2b**, and the sums of ΔH values for all transitions of **3a** and **3b** are less than for **2a** and **2b**. This shows that the end chains and spacer chains of **3a** and **3b** are highly disordered in the crystal phase, so that the gain in entropy of melting, of mesophase changes, and of isotropization is small.

The *d* spacings of (dimethylamino)stilbene **12** in the orthorhombic crystalline state increase with increasing temperature and are greater than the calculated molecular length (~27.8 Å), and there are two molecules per unit cell. The *d* spacings of [(hexyloxy)piperidino]stilbene **13** at 177 and 165 °C in the S_A and S_B phases, respectively, are smaller than the calculated molecular length (~37.5 Å) as shown in Table IV. This can be explained by the conformation of the mesogen having an angle of about 160° between the axis of the stilbene and the axis of the (hexyloxy)piperidine calculated by molecular modeling.

The approximate mode of packing of copolysiloxanes **2b** and **3b** in the smectic A phase is evident from small-angle X-ray diffraction peaks. Several studies[60–64] on the X-ray diffraction of some SCLC polysiloxanes found *d* spacings much smaller than twice the calculated side chain length. For a smectic A phase, this is often explained by interdigitated bilayer structure with the overlap of the polarizable side chains, as shown in Figure 13.

We cannot rule out the possibility that the assigned orthorhombic crystalline structures are S_E phases. Like the orthorhombic crystalline structure, the powder X-ray diffraction pattern of the S_E phase also shows three peaks in the wide-angle region corresponding to the 110, 200, and 210 reflections. Sutherland and Ali-Adib[65] also observed these three reflections below the S_A phase of terminally bromo-substituted SCLC polysiloxanes and interpreted it as either an S_E phase or an orthorhombic crystal.

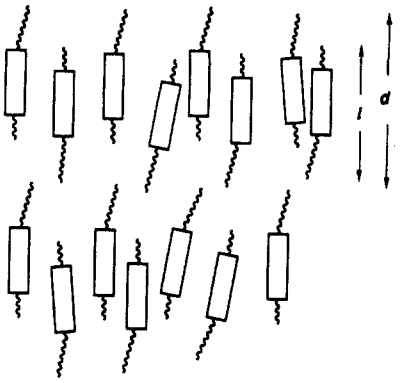

Figure 13. Schematic representation of the molecular packing of polymer **3b**. The molecules have a 162° angle between the axis of the C_{11} chain and the stilbene plane according to molecular model calculations.

Monolayers. The mean molecular area per repeat unit of homopolysiloxane **2a** corresponds to the expected value of a close-packed array of benzene rings perpendicular to the water surface. The isotherm of **2a** is like the Π–A isotherm of 4-cyano-4′-*n*-pentyl-*p*-terphenyl[66] in which the monolayer collapses at 22 mN/m with an average molecular area of 23 Å^2. However, the 30–34-Å^2 mean molecular areas of polysiloxanes **2b**, **3a**, and **3b** are more like those of alkylcyanobiphenyl monolayers.[67] Unlike cyanobiphenyls and fatty acids, the [(hexyloxy)piperidino]stilbene polymers **3a** and **3b** have no polar end that can hydrogen bond to the water surface and leave the more lipophilic part of the structure above the water. Hydrogen bonding of the amine group of **3a** or **3b** to the water would require that the stilbene and piperidine rings be parallel to the surface. We presume that the hydrophobic spacer chains and polysiloxane backbones avoid water, but the orientations of the amine, stilbene, and ester groups with respect to the water are not known. Due to its low surface energy the poly(dimethylsiloxane) backbone is probably in contact with air.

The monolayers of side chain copolysiloxanes **2b** and **3b** are more stable than those side chain homopolysiloxanes **2a** and **3a**. Figures 9 and 10 show the expected decrease in Mma of **2a** and **3a** at constant pressure and unusual increases of Mma of the monolayers of **2b** and **3b** after 40–80 min, which might be due to temperature fluctuations or to rearrangement of the main chains or side chains. The discontinuity observed at about 53 mN/m in the Π–*A* isotherm of **2b** might also be due to reorientation of the main chains or side chains into a more tightly packed arrangement. Since the unusual isotherm of **2b** was reproducible, it is not likely due to temperature variations, but to relaxation into a more stable monolayer structure.

The UV spectra of LB layers of **2b** and **3b** are much different from one another. That of **2b** (Figure 11) shows only a shoulder instead of the usual long-wavlength absorbance maximum of the (dimethylamino)stilbene-carboxylate at 375–392 nm in various solvents (the spectra are solvatochromic) and at 395 nm in a spin-coated film of polyacrylate **1**. Therefore, in the LB film the transition moment and the long axis of the stilbene must be oriented mainly orthogonal to the substrate surface. The spectrum of **3b** (Figure 12) shows an absorbance maximum blue

shifted to 336 nm, compared with 368–382 nm in various solutions. The blue shift seen in analogous monomeric LB films has been attributed to H-aggregates.[68] The strong 336-nm absorption indicates that **3b** is not oriented orthogonal to the substrate.

Conclusion

The variety of phases found in polymers **2a**, **2b**, **3a**, and **3b** should make possible study of their nonlinear optical properties as a function of molecular packing in oriented crystal phases of spin-coated thin films obtained by electric field poling and in oriented Langmuir–Blodgett multilayers.

Acknowledgment. We thank Dr. Cristopher M. Adams for the molecular modeling, Dr. Matthias Naumann for help with the X-ray and microscopy experiments, and Angela Thibodeaux for her help with the LB experiments. This research was supported in part by the Office of Naval Research (W.T.F.) and the donors of the Petroleum Research Fund, administered by the American Chemical Society (R.S.D.).

References and Notes

(1) Prasad, P. N.; Williams, D. J. *Introduction to Nonlinear Optical Effects in Molecules and Polymers*; John Wiley & Sons, Inc.: New York, 1991.
(2) Small, R. D.; Singer, K. D.; Sohn, J. E.; Kuzyk, M. G.; Lalama, S. J. *Proc. SPIE* **1986**, *682*, 160–169.
(3) Singer, K. D.; Sohn, J. E.; Lalama, S. J. *Appl. Phys. Lett.* **1986**, *49*, 248–250.
(4) Hampsch, H. L.; Yang, J.; Wong, G. K.; Torkelson, J. M. *Macromolecules* **1988**, *21*, 526–528.
(5) Hampsch, H. L.; Yang, J.; Wong, G. K.; Torkelson, J. M. *Polym. Commun.* **1989**, *30*, 40–43.
(6) Hampsch, H. L.; Torkelson, J. M.; Bethke, S. J.; Grubb, S. G. *J. Appl. Phys.* **1990**, *67*, 1037–1041.
(7) Hampsch, H. L.; Yang, J.; Wong, G. K.; Torkelson, J. M. *Mater. Res. Soc. Symp. Proc.* **1990**, *173*, 625–630.
(8) Ye, C.; Marks, T. J.; Yang, J.; Wong, G. K. *Macromolecules* **1987**, *20*, 2322–2324.
(9) Ye, C.; Minami, N.; Marks, T. J.; Yang, J.; Wong, G. K. *Macromolecules* **1988**, *21*, 2899–2901.
(10) Dai, D.-R.; Marks, T. J.; Yang, J.; Lundquist, P. M.; Wong, G. K. *Macromolecules* **1990**, *23*, 1891–1894.
(11) Eich, M.; Sen, A.; Looser, H.; Bjorklund, G. C.; Swalen, J. D.; Twieg, R.; Yoon, D. Y. *J. Appl. Phys.* **1989**, *66*, 2559–2567.
(12) Nijhuis, S.; Rikken, G. L. J. A.; Havinga, E. E.; ten Hoeve, W.; Wynberg, H.; Meijer, E. W. *J. Chem. Soc., Chem. Commun.* **1990**, 1093–1094.
(13) Rikken, G. L. J. A.; Seppen, C. J. E.; Nijhuis, S.; Meijer, E. W. *Appl. Phys. Lett.* **1991**, *58*, 435–437.
(14) Hubbard, M. A.; Marks, T. J.; Yang, J.; Wong, G. K. *Chem. Mater.* **1989**, *1*, 167–169.
(15) Park, J.; Marks, T. J.; Yang, J.; Wong, G. K. *Chem. Mater.* **1990**, *2*, 229–231.
(16) Eich, M.; Reck, B.; Yoon, D. Y.; Willson, C. G.; Bjorklund, G. C. *J. Appl. Phys.* **1989**, *66*, 3241–3247.
(17) Jungbauer, D.; Reck, B.; Twieg, R.; Yoon, D. Y.; Willson, C. G.; Swalen, J. D. *Appl. Phys. Lett.* **1990**, *56*, 2610–2612.
(18) Jungbauer, D.; Teraoka, I.; Yoon, D. Y.; Reck, B.; Swalen, J. D.; Twieg, R.; Willson, C. G. *J. Appl. Phys.* **1991**, *69*, 8011–8017.
(19) Mandal, B. K.; Kumar, J.; Huang, J.-C.; Tripathy, S. *Makromol. Chem., Rapid Commun.* **1991**, *12*, 63–68.
(20) Mandal, B. K.; Chen, Y. M.; Lee, J. Y.; Kumar, J.; Tripathy, S. *Appl. Phys. Lett.* **1991**, *58*, 2459–2460.
(21) Mandal, B. K.; Jeng, R. J.; Kumar, J.; Tripathy, S. K. *Makromol. Chem., Rapid Commun.* **1991**, *12*, 607–612.
(22) McArdle, C. B., Ed. *Side Chain Liquid Crystal Polymers*; Blackie and Sons: Glasgow, U.K., 1989.
(23) Griffin, A. C.; Bhatti, A. M.; Hung, R. S. L. *Proc. SPIE* **1986**, *682*, 65–69.
(24) Stamatoff, J. B.; Buckley, A.; Calundann, G.; Choe, E. W.; DeMartino, R.; Khanarian, G.; Leslie, T.; Nelson, G.; Stuetz, D.; Teng, C.-C.; Yoon, H.-N. *Proc SPIE* **1986**, *682*, 85–92.
(25) Le Barny, P.; Ravaux, G.; Dubois, J. C.; Parneix, J. P.; Njeumo, R.; Legrand, C.; Levelut, A. M. *Proc. SPIE* **1986**, *682*, 56–64.
(26) Leslie, T. M.; DeMartino, R. N.; Choe, E. W.; Khanarian, G.; Haas, D.; Nelson, G.; Stamatoff, J. B.; Stuetz, D. E.; Teng, C.-C.; Yoon, H.-N. *Mol. Cryst. Liq. Cryst.* **1987**, *153*, 451–477.
(27) DeMartino, R. N.; Choe, E. W.; Khanarian, G.; Haas, D.; Leslie, T.; Nelson, G.; Stamatoff, J.; Stuetz, D.; Teng, C. C.; Yoon, H. In *Nonlinear Optical and Electroactive Polymers*; Prasad, P. N., Ulrich, D. R., Eds.; Plenum Press: New York, 1988; pp 169–186.
(28) Esselin, S.; Le Barny, P.; Robin, P.; Broussoux, D.; Dubois, J. C.; Raffy, J.; Pocholle, J. P. *Proc. SPIE* **1988**, *971*, 120–127.
(29) Griffin, A. C.; Bhatti, A. M.; Hung, R. S. L. In *Nonlinear Optical and Electroactive Polymers*; Prasad, P. N., Ulrich, D. R., Eds.; Plenum Press: New York, 1988; pp 375–391.
(30) McCulloch, I. A.; Bailey, R. T. *Proc. SPIE* **1989**, *1147*, 134–140.
(31) Ore, F. R., Jr.; Hayden, L. M.; Sauter, G. F.; Pasillas, P. L.; Hoover, J. M.; Henry, R. A.; Lindsay, G. A. *Proc. SPIE* **1989**, *1147*, 26–35.
(32) Pfeiffer, M.; Haase, W. *Proc. SPIE* **1990**, *1337*, 234–245.
(33) Nijhuis, S.; Rikken, G. L. J. A.; Havinga, E. E.; ten Hoeve, W.; Wynberg, H.; Meijer, E. W. *J. Chem. Soc., Chem. Commun.* **1990**, 1093–1094.
(34) Rikken, G. L. J. A.; Seppen, C. J. E.; Nijhuis, S.; Meijer, E. W. *Appl. Phys. Lett.* **1991**, *58*, 435–437.
(35) Zhao, M.; Bautista, M.; Ford, W. T. *Macromolecules* **1991**, *24*, 844–849.
(36) Ford, W. T.; Bautista, M.; Zhao, M.; Reeves, R. J.; Powell, R. C. *Mol. Cryst. Liq. Cryst.* **1991**, *198*, 351–356.
(37) Robello, D. R. *J. Polym. Sci., Part A: Polym. Chem.* **1990**, *28*, 1–13.
(38) Further details are in the Ph.D. Dissertation of M. O. Bautista, Oklahoma State University, 1992.
(39) Gray, G. W.; Hawthorne, W. D.; Lacey, D.; White, M. S.; Semlyen, J. A. *Liq. Cryst.* **1989**, *6*, 503–513.
(40) McManus, J. M.; McFarland, J. W.; Gerber, C. F.; McLamore, W. M.; Laubach, G. D. *J. Med. Chem.* **1965**, *8*, 766–776.
(41) Takai, Y.; Shibata, Y. Jpn. Kokai Tokkyo Koho JP 63 101 350, 1988; *Chem. Abstr.* **1988**, *109*, 129828.
(42) Gray, G. W.; Lacey, D.; Nestor, G.; White, M. S. *Makromol. Chem., Rapid Commun.* **1986**, *7*, 71–76.
(43) deMarignan, G.; Teyssie, D.; Boileau, S.; Malthete, J.; Noel, C. *Polymer* **1988**, *29*, 1318–1322.
(44) Suzuki, T.; Okawa, T.; Ohnuma, T.; Sakon, Y. *Makromol. Chem., Rapid Commun.* **1988**, *9*, 755–760.
(45) Lee, M. S, K.; Gray, G. W.; Lacey, D.; Toyne, K. J. *Makromol. Chem., Rapid Commun.* **1989**, *10*, 325–331.
(46) Duran, R.; Strazielle, C. *Macromolecules* **1987**, *20*, 2853–2858.
(47) Doucet, J.; Levelut, A. M.; Lambert, M.; Liebert, L.; Strzelecki, L. *J. Phys. Suppl.* **1975**, *36*, C1–13.
(48) Friedzon, Y. S.; Boiko, N. I.; Shibaev, V. P.; Plate, N. A. As reported by Noel, C. In *Side Chain Liquid Crystal Polymers*; McArdle, C. B., Ed.; Blackie and Sons: Glasgow, U.K., 1989; p 184.
(49) Nestor, G.; White, M. S.; Gray, G. W.; Lacey, D.; Toyne, K. J. *Makromol. Chem.* **1987**, *188*, 2759–2767.
(50) Lang, P.; Burchard, W. *Makromol. Chem., Rapid Commun.* **1987**, *8*, 451–455.
(51) Sagane, T.; Lenz, R. W. *Polym. J.* **1988**, *20*, 923–931.
(52) Sagane, T.; Lenz, R. W. *Polymer* **1989**, *30*, 2269–2278.
(53) Sagane, T.; Lenz, R. W. *Macromolecules* **1989**, *22*, 3763–3767.
(54) Percec, V.; Lee, M. *Macromolecules* **1991**, *24*, 1017–1024.
(55) Stevens, H.; Rehage, G.; Finkelmann, H. *Macromolecules* **1984**, *17*, 851–856.
(56) Gray, G. W.; Hawthorne, W. D.; Hill, J. S.; Lacey, D.; Lee, M. S. K.; Nestor, G.; White, M. S. *Polymer* **1989**, *30*, 964–971.
(57) Percec, V.; Keller, A. *Macromolecules* **1990**, *23*, 4347–4350.
(58) Dave, J. S.; Patel, P. R. *Mol. Cryst.* **1966**, *2*, 103–114.
(59) Demus, D.; Diele, S.; Grande, S.; Sackmann, H. In *Advances in Liquid Crystals*; Brown, G. H., Ed.; Academic Press: New York, 1983; Vol. 6, pp 1–107.
(60) Keller, K. N. *Macromolecules* **1989**, *22*, 4597–4599.
(61) Davidson, P.; Levelut, A. M.; Achard, M. F.; Hardouin, F. *Liq. Cryst.* **1989**, *4*, 561–571.
(62) Noel, C. In *Side Chain Liquid Crystal Polymers*; McArdle, C. B., Ed.; Blackie and Sons: Glasgow, U.K., 1989; pp 159–195.
(63) Tinh, N. H.; Achard, M. F.; Hardouin, F.; Mauzac, M.; Richard, H.; Sigaud, G. *Liq. Cryst.* **1990**, *7*, 385–394.
(64) Sutherland, H. H.; Ali-Adib, Z.; Gray, G. W.; Lacey, D.; Nestor, G.; Toyne, K. J. *Liq. Cryst.* **1988**, *3*, 1293–1300.
(65) Sutherland, H. H.; Ali-Adib, Z. *Liq. Cryst.* **1991**, *9*, 899–902.
(66) Daniel, M. F.; Lettington, O. C.; Small, S. M. *Thin Solid Films* **1983**, *99*, 61–69.
(67) Daniel, M. F.; Lettington, O. C.; Small, S. M. *Mol. Cryst. Liq. Cryst.* **1983**, *96*, 373–385.
(68) Umemura, J.; Hishiro, Y.; Kawai, T.; Takenaka, T.; Gotoh, Y.; Fujihira, M. *Thin Solid Films* **1989**, *178*, 281–287.